HHS Public Access

Author manuscript

Nature. Author manuscript; available in PMC 2012 December 13.

Published in final edited form as:

Nature. 2012 November 15; 491(7424): 449–453. doi:10.1038/nature11624.

A UV-independent pathway to melanoma carcinogenesis in the redhair-fairskin background

Devarati Mitra[1], **Xi Luo**[2], **Ann Morgan**[1], **Jin Wang**[3], **Mai P. Hoang**[4], **Jennifer Lo**[1], **Candace R. Guerrero**[3], **Jochen K. Lennerz**[5], **Martin C. Mihm**[4], **Jennifer A. Wargo**[6], **Kathleen C. Robinson**[1], **Suprabha P. Devi**[1], **Jillian C. Vanover**[7], **John A. D'Orazio**[7], **Martin McMahon**[8], **Marcus W. Bosenberg**[9], **Kevin M. Haigis**[2], **Daniel A. Haber**[2], **Yinsheng Wang**[3], and **David E. Fisher**[1,*]

[1]Cutaneous Biology Research Center, Massachusetts General Hospital, Charlestown, Massachusetts 02129, USA

[2]Massachusetts General Hospital Cancer Center, Charlestown, Massachusetts 02129, USA

[3]Department of Chemistry, University of California, Riverside, California 92521, USA

[4]Department of Pathology, Massachusetts General Hospital, Boston, Massachusetts 02114, USA

[5]Institute of Pathology, University Ulm, Ulm 89070, Germany

[6]Department of Surgery, Massachusetts General Hospital, Boston, Massachusetts 02114, USA

[7]Markey Cancer Center, University of Kentucky School of Medicine, Lexington, Kentucky 40536, USA

[8]Helen Diller Family Comprehensive Cancer Center, University of California San Francisco, San Francisco, California 94143, USA

[9]Department of Dermatology, Yale University School of Medicine, New Haven, Connecticut 06520, USA

Abstract

People with pale skin, red hair, freckles, and an inability to tan—the "redhair/fairskin" phenotype — are at highest risk of developing melanoma, compared to all other pigmentation types[1]. Genetically, this phenotype is frequently the product of inactivating polymorphisms in the

Correspondence and requests for materials should be addressed to D.E.F. (dfisher3@partners.org).

Supplementary Information is linked to the online version of the paper at www.nature.com/nature.

The authors declare no competing financial interests.

Author Contributions

D.M. and D.E.F. conceived and planned the project. M.M., M.W.B., and K.M.H., provided the mice carrying the *PTEN, BRAF*^{V600E} and Tyr-Cre(ER)^{T2} alleles. D.M. performed the mouse work with help from A.M., J.L., S.D. and K.C.R.. Histology was performed by D.M., X.L., J.C.V. and J.A.D. with support from D.A.H.. Pathological analysis was provided by M.H., J.K.L. and M.C.M.. *In vitro* studies were performed by D.M. with help from A.M. and J.L.. J.A.W. generated the primary mouse cell line. J.W., C.G. and Y.W. collected DNA from mouse skin and performed LC-MS/MS/MS. The manuscript was written by D.M. and D.E.F.. All authors discussed the results and commented on the manuscript.

Melanocortin 1 receptor (*MC1R*) gene. *MC1R* encodes a cAMP stimulating G-protein coupled receptor that controls pigment production. Minimal receptor activity, as in redhair/fairskin polymorphisms, produces red/yellow pheomelanin pigment, while increasing MC1R activity stimulates production of black/brown eumelanin[2]. Pheomelanin has weak UV shielding capacity relative to eumelanin and has been shown to amplify UVA-induced reactive oxygen species (ROS) [3–5]. Several observations, however, complicate the assumption that melanoma risk is completely UV dependent. For example, unlike non-melanoma skin cancers, melanoma is not restricted to sun-exposed skin and UV signature mutations are infrequently oncogenic drivers[6]. While linkage of melanoma risk to UV exposure is beyond doubt, UV-independent events are also likely to play a significant role[1,7]. Here, we introduced into mice carrying an inactivating mutation in the *Mc1r* gene (who exhibit a phenotype analogous to redhair/fairskin humans), a conditional, melanocyte-targeted allele of the most commonly mutated melanoma oncogene, $BRaf^{V600E}$. We observed a high incidence of invasive melanomas without providing additional gene aberrations or UV exposure. To investigate the mechanism of UV-independent carcinogenesis, we introduced an albino allele, which ablates all pigment production on the $Mc1r^{e/e}$ background. Selective absence of pheomelanin synthesis was protective against melanoma development. In addition, normal $Mc1r^{e/e}$ mouse skin was found to have significantly greater oxidative DNA and lipid damage than albino-$Mc1r^{e/e}$ mouse skin. These data suggest that the pheomelanin pigment pathway produces UV-independent carcinogenic contributions to melanomagenesis by a mechanism of oxidative damage. While UV protection remains important, additional strategies may be required for optimal melanoma prevention.

To study the role of pigmentation in $BRaf^{V600E}$ melanoma development, we utilized a series of genetically matched mice on the C57BL/6 background with various pigmentation phenotypes (Fig. 1a). To mimic dark-skinned individuals with a high eumelanin-to-pheomelanin ratio, we used mice with the wild type C57BL/6 pigmentation phenotype ("black"). To mimic individuals with the redhair/fairskin phenotype who carry a high pheomelanin-to-eumelanin ratio, we used mice with premature termination of the *Mc1r* transcript ($Mc1r^{e/e}$, "red")[8]. To mimic individuals with albinism who have no melanin, we used mice with an inactivating mutation at the *Tyrosinase* locus ($Tyr^{c/c}$, "albino")[9]. Since tyrosinase is the initial and rate-limiting enzyme in melanin synthesis, albino melanocytes do not produce any pigment, but are normal in number and viability[10].

We generated two variants of each pigmentation phenotype. One variant contains melanocytes in the dermis. A second matched variant contains transgenic Stem Cell Factor expressed under the keratin 14 promoter ("*K14-SCF*"), which mimics SCF expression in human epidermal keratinocytes and results in epidermal melanocyte localization[11].

To create a genetic context primed for the induction of melanoma we also introduced into each of our 6 variants, a previously published system for inducible, melanocyte-specific expression of oncogenic $BRaf^{V600E}$ [12]. In humans, mice and zebrafish, expression of $BRaf^{V600E}$ in melanocytes primarily causes benign nevi, rather than melanoma[12–15]. In this context, malignant melanoma progression is thought to be constrained by oncogene-induced senescence[15]. Consistent with this, expression of $BRAF^{V600E}$ in conjunction with silencing of *PTEN*, *TP53* or *CDKN2A* leads to development of malignant melanoma[12–14].

Spontaneous progression of BRaf^{V600E}-expressing melanocytes to malignant melanoma has been reported, however, following a long latency period in C57BL/6 mice, though this phenomenon was not seen on an outbred model[12,16,17].

We initially produced 6 groups of BRaf^{V600E} inducible ("*BRaf^{CA}*") mice representing 3 pigmentation variants ("black," "red," and "albino") with or without epidermal melanocytes (+/− *K14-SCF*, Fig. 1b). Melanocyte-selective expression of BRaf^{V600E} was achieved by tamoxifen-mediated activation of Cre recombinase (*Tyr-Cre(ER)^{T2}*) in adult mice carrying the *BRaf^{CA}* allele. The animals were then followed without environmental genotoxic stressors (such as UV). Black and albino BRaf^{CA} mice developed similarly low rates of melanoma after a long latency (regardless of *K14-SCF* status). In contrast, red BRaf^{CA} mice developed melanomas at an accelerated rate with >50% having tumors after one year, regardless of *K14-SCF* status (Fig. 1c and 1d).

The tumors on the black, red and albino backgrounds were grossly amelanotic and largely on the dorsal trunk (within the tamoxifen-treated areas). Occasionally, a tumor would develop on the ventral trunk, tail or paw, which may reflect a predictable spread of tamoxifen secondary to grooming. (Fig. 2a, 2b and 2c). The tumors, which were primarily dermal, were generally amelanotic on the red and albino backgrounds, whereas the melanomas in black mice often exhibited superficial pigmentation adjacent to the epidermis (Fig. 2d, 2e and 2f). Regardless of pigmentation background, the tumors were histologically similar with spindle cell features which were not easily distinguishable from tumors on C57BL/6 *BRaf^{CA}-Pten$^{flox/flox}$* animals generated in parallel (Fig. 2 vs. Supplementary Fig. 1). Upon closer examination, occasional red-BRaf^{V600E} tumor cells were found to contain melanin (Fig. 2g and 2h). It was further possible to increase pigmentation in the most superficial melanoma cells with topical application of forskolin, an adenylate cyclase agonist known to stimulate skin pigmentation[18] (Fig. 2i). The limited induction of pigmentation is likely related to forskolin's poor tissue penetration, but nonetheless demonstrates the ability of the melanoma cells to become hyper-pigmented *in vivo* upon activation of cAMP signaling.

Tumors on all three pigmentation backgrounds stained positively for S100, a standard immunohistochemical melanoma marker (Fig. 2j). In addition, RT-PCR revealed that the tumors consistently express the melanocytic pigment genes *M-Mitf, Dct, Tyrp1*, and *Tyr* (Fig. 3a, 3d and data not shown). In addition, occasional Hmb45+ cells could be found by immunofluorescence (Supplementary Fig. 2). The tumors on all three pigmentation backgrounds were locally invasive to fat and skeletal muscle with active mitoses. While no gross visceral organ metastases were observed, small clusters of cells expressing gp100, the premelanosome-associated glycoprotein (Pmel/gp100/Hmb45), could be found in skin draining lymph nodes (Fig. 2k).

Utilizing a primary cell line derived from one of the red mouse melanomas, we observed that forskolin upregulated the expression of the melanocyte-specific isoform of *Mitf* (M-Mitf), and produced a dramatic increase in expression of the *Dct* and *Tyrp1* pigment genes, consistent with the ability of the cells to respond to melanocytic differentiation signals (Fig. 3a).

To determine if the melanoma cells were dependent on the presumed oncogenic driver $BRaf^{V600E}$, we tested their response to small molecule inhibitors of BRAF or MEK. Treatment with the oncogenic BRAF inhibitor, PLX4720, or the MEK inhibitor, U0126, prevented melanoma cell proliferation *in vitro,* and PLX4720 blocked tumor cell growth *in vivo,* consistent with a dependency of these tumors on the $BRaf^{V600E}$ oncoprotein (Fig. 3b and 3c). BRaf inhibition also elevated the expression of melanocytic genes as previously reported in human melanomas (Fig. 3d)[19].

Since inactivating mutations in *Mc1r* alter cAMP levels in the cell, red mice undoubtedly have numerous intracellular pathway differences relative to wild-type $Mc1r^{E/E}$ (black) animals, including altered DNA repair[20]. We therefore wished to study whether the pheomelanin pigment pathway itself plays an intrinsic mechanistic role, or whether it is merely a marker of melanoma risk. To investigate this question we introduced the albino tyrosinase ($Tyr^{c/c}$) allele into the red $Mc1r^{e/e}$ background to test melanoma incidence in albino-$Mc1r^{e/e}$ animals, which retain low Mc1r activity and also lack all pigment production (Fig. 4a). A melanocyte-targeted *LacZ* transgene was used to confirm that the albino allele does not alter melanocyte number in these mice (Supplementary Fig. 3a and 3b)[10]. As shown in Figure 4b, the albino allele profoundly protected red mice from melanoma. The rare albino-$Mc1r^{e/e}$ melanomas occurred after long latency and exhibited the same amelanotic, S100+, histologic features as the other pigmentation variant $BRaf^{CA}$ animals (Supplementary Fig. 4a, 4b and 4c). This observation suggests that the pheomelanin synthesis pathway is necessary for the high rate of UV-independent melanoma in the red mice.

Prior studies have demonstrated that UV radiation amplifies ROS production and subsequent oxidative DNA damage in the skin of pigmented mice[21]. UV radiated cells with high pheomelanin levels have been found to carry particularly high levels of oxidative damage[4,5]. Since darkly pigmented individuals carry both pheomelanin and eumelanin, it has been hypothesized that their lower melanoma risk may result from eumelanin intermediates and polymers absorbing ROS and functioning as *in vivo* antioxidants[22,23].

To determine if ROS-mediated oxidative DNA damage is affected by the pheomelanin synthesis pathway, levels of 8,5′-cyclo-2′-deoxyadenosine (cdA) and 8,5′-cyclo-2′-deoxyguanosine (cdG) were measured in DNA isolated from skin of red-$Mc1r^{e/e}$ and albino-$Mc1r^{e/e}$ mice, using a previously reported LC-tandem mass spectrometric method[24] (Fig. 4c). These two ROS-mediated cyclopurines are unlikely to be artificially induced during sample preparation and are quite stable[25,26]. Significantly, replication studies in *E. coli* have shown that *S*-cdA and *S*-cdG can lead to A to T and G to A mutations at frequencies of 11% and 20%, respectively[27]. Comparing cyclopurine levels in the skin of various pigmentation variant mice, it was found that the levels of cdA and cdG are significantly higher in skin from red-$Mc1r^{e/e}$ mice as compared to skin from albino-$Mc1r^{e/e}$ animals (Fig. 4d, 4e). This observation suggests that activation of the pheomelanin synthesis pathway results in increased oxidative DNA damage. Correlative evidence for increased cellular oxidative stress was also found in the observation that red-$Mc1r^{e/e}$ mouse skin carries higher levels of lipid peroxides, a product of ROS-mediate lipid damage (Fig 4f).

The findings reported here suggest that in the context of oncogenic BRAF activation, individuals carrying redhair/fairskin *MC1R* polymorphisms have an increased risk of melanoma, due to both poor protection from environmental carcinogens like UV radiation, and also via intrinsic carcinogenic features of pheomelanin synthesis; potentially via pheomelanin itself, an intermediate of pigment synthesis or a by-product of the pathway.

In humans, there are multiple *MC1R* polymorphisms with varied perturbation of receptor function that produce a redhair/fairskin phenotype, however, a unifying feature of these various polymorphisms is a high pheomelanin to eumelanin ratio, which is also produced by the $Mc1r^{e/e}$ allele in mice. Recent data from Noonan et al intriguingly demonstrated that UV irradiated black animals over-expressing HGF are at higher risk of melanoma than their albino counterparts[21]. While the present study revealed a small difference between black and albino BRAF(V600E) driven melanomas in the presence of *K14-SCF* (Fig 1d), the effect did not reach statistical significance (p=0.103), perhaps signifying oncogene specific differences. It seems likely that the effects of pigmentation and UV radiation are likely to work together in determining melanoma risk.

The photometer used for our lab's routine calibration (International Light 1400) was unable to detect any measurable UV radiation in our mouse cages during ambient light exposure. However, strong epidemiological work links UV radiation to melanoma, and the current data do not diminish the importance of sun exposure as a key contributing factor[1]. In humans, it is likely the UV-independent effects act in concert with UV-mediated cellular toxicity. In agreement with published studies, UV radiation at a UVA/UVB ratio similar to that found in sunlight (10J/cm^2 UVA and 0.65J/cm^2 UVB) was found to exacerbate oxidative damage selectively in red mouse skin as measured by levels of lipid peroxidation[4,5] (Supplementary Fig. 5a). Studies are underway to investigate whether UV radiation is able to alter the red-$BRaf^{V600E}$ tumor phenotype. Preliminary studies examining the effect of visible light (180J/cm^2) did not reveal significantly altered lipid peroxidation in any pigmentation context (p=0.4506). Perhaps, however, there is a trend towards an increased level of lipid peroxidation in red mouse skin (Supplementary Fig. 5b).

Further evidence suggesting a UV-independent redhair/fairskin melanoma risk is the observation that while darker-skinned individuals have a significantly lower risk of melanoma than lighter-skinned individuals, the sun protective factor (SPF, a measurement of sunburn protection) of darker skin has been estimated at only in the range of SPF 2.0–4.0[28]. In addition, sunscreen (typically SPF 20–40) has exhibited weak efficacy in protecting against melanoma, unlike its protection against cutaneous squamous cell carcinoma[29,30]. There are numerous potentially explanations for the sunscreen-melanoma data, however it is also possible that UV shielding may protect against only one of several carcinogenic mechanisms—with the intrinsic pheomelanin pathway representing an additional contributor to melanomagenesis via UV-independent means. These data do not argue against a role for UV in melanomagenesis. Indeed the effect of UV likely exacerbates this mechanism, such that UV shielding and sunscreen remain extremely important for skin cancer prevention. However, additional preventative strategies may be essential to optimally diminish melanoma risk in the most susceptible individuals.

METHODS SUMMARY

Mice

At 6–10 weeks of age, mice were treated topically with 20mg/ml tamoxifen for 5 days. For topical darkening, 20% coleus extract was applied as previously described[17]. For *in vivo* PLX4720 studies, animals were given *ad libitum* mouse chow containing 2% PLX4720 by weight. All studies and procedures involving animal subjects were approved by the Institutional Animal Care and Use Committees of Massachusetts General Hospital and Dana-Farber Harvard Cancer Center, and were conducted strictly in accordance with the approved animal handling protocol.

Morphological examination

Histology and immunostaining were performed according to established protocols using S100 (Dako), DCT (Santa Cruz), C5 MITF (tissue culture supernatant), HMB45 (Santa Cruz), and gp100 (Abcam) antibodies.

Primary Cell Culture

Primary tumor was digested overnight and grown in DMEM. Proliferation was measured by the CellTiter-Glo Luminescent Cell Viability Assay (Promega).

Quantitative RT-PCR

mRNA expression of melanocytic markers was determined using intron-spanning mouse-specific primers with SYBR FAST qPCR master mix (Kapa Biosystems).

Measurement of 8,5′-Cyclopurine-2′-deoxynucleosides

8,5′-cyclo-2′-deoxyadenosine (cdA) and 8,5′-cyclo-2′-deoxyguanosine (cdG) levels were measured as previously published[24]. Briefly, nuclear DNA was isolated from mouse skin, digested to nucleosides, separated by HPLC and analyzed by LC-MS/MS/MS.

Measurement of Lipid Peroxidation

Mouse skin was irradiated with UV (10J/cm^2 UVA-0.65J/cm^2 UVB), or visible light (180 J/cm^2). After homogenization, lipid peroxidation was measured with the OxiSelect TBARS Assay Kit (Cell Biolabs).

FULL METHODS

Mice

All animals used for breeding were backcrossed a minimum of 6 generations onto the C57BL/6 genetic background (this corresponds to a >98.4% C57BL/6 congenic animal, http://jaxmice.jax.org/support/nomenclature/tutorial.html). The black (wild type), red (*Mc1r$^{e/e}$*) and albino (*Tyr$^{c/c}$*) animals were purchased from Jackson Laboratories. *K14-SCF* animals were acquired from T. Kunisada. Genotyping of each litter, including the *Tyr-Cre(ER)^{T2}*, *BRaf^{CA}*, and *PTEN$^{flox/flox}$* alleles was performed as previously published[10,11]. At 6–10 weeks of age the dorsal fur was trimmed using animal shears with a 0.25 mm head and

the mice were treated topically with 20 mg/ml tamoxifen for 5 consecutive days. For tumor darkening, a 20% solution of *Coleus forskohlii* root extract (80 μM forskolin) was topically applied daily as previously described[17]. For *in vivo* PLX4720 studies, animals were given *ad libitum* mouse chow containing 2% PLX4720 by weight or control chow acquired from Plexxikon Inc. All studies and procedures involving animal subjects were approved by the Institutional Animal Care and Use Committees of Massachusetts General Hospital and Dana-Farber Harvard Cancer Center and were conducted strictly in accordance with the approved animal handling protocol.

Dissection and histology

Tissues of interest were photographed, excised, weighed, rinsed in phosphate-buffered saline (PBS), fixed in 10% neutral-buffered formalin, rinsed in PBS, and stored in 70% ethanol. Formalin-fixed tissues were paraffin embedded (FFPE) and sectioned (3–5 μm) using standard procedures. Morphological analysis was performed using multiple independent samples per site/organ (5 to 9 samples per genotype) as well as >6 animals. Two pathologists (JKL, MPH) independently examined the histopathology of the tumor samples. Digitization and image capture was performed using an Olympus DP70 digital camera (Olympus, Tokyo, Japan) connected to an Olympus BX51 light microscope or a Scanscope whole-slide scanning system (Aperio, Vista, CA).

Immunohistochemistry

For immunohistochemistry, sections were deparaffinized with xylene and hydrated with a graded series of alcohol. Sections were boiled in 50 mM TRIS-buffer (pH9) or citrate for antigen retrieval and rinsed in PBS. Sections were blocked in 1% BSA, 0.1% Triton X-100 PBS, incubated with 1:200 dilutions of rabbit anti-S100 (Dako), 1:100 dilutions of goat anti-DCT (Santa Cruz), 1:200 dilutions of mouse-anti HMB45 (Santa Cruz) and 1:200 dilutions of mouse-anti gp100 (Abcam) antibodies, followed by visualization with appropriate secondary antibodies conjugated to Alexa594 or Alexa488 (1:500). Appropriate controls for specificity of staining were included and images were captured using an upright fluorescence microscope (Eclipse 90i, Nikon). To identify epidermal melanocytes, skin from reporter mice carrying the various pigmentation alleles and the *K14-SCF* transgene as well as a *DCT-LacZ* reporter allele was cryosectioned and stained with XGal and nuclear fast red counterstaining.

Primary Cell Culture

Tumor cells were digested overnight in 10 mg/ml collagenase and 1 mg/ml hyaluronidase. Initially tumor cells were grown in RPMI media with HEPES and 20% serum. Subsequently tumor cells were grown in DMEM media with 10% serum. Proliferation after 72 hours of PLX4720 (Chemietek) and U0126 (Cell Signaling) was determined by the CellTiter-Glo Luminescent Cell Viability Assay (Promega).

Quantitative RT-PCR

RNA was harvested from primary cultured tumor cells treated for varying times with forskolin or PLX4720 using the RNeasy Plus mini kit (Qiagen). mRNA expression of

melanocytic markers was determined using intron-spanning mouse-specific primers with Kapa SYBR FAST qPCR master mix (Kapa Biosystems). Expression was normalized to 18s rRNA and 0 hour time-points. Primer sequences used: Mitf fwd GCCTGAAACCTTGCTATGCTGGAA, Mitf rev- AAGGTACTGCTTTACCTGGTGCCT, Dct fwd- AGGTACCATCTGTTGTGGCTGGAA, Dct rev- AGTTCCGACTAATCAGCGTTGGGT, Tyrp1 fwd-TGGGGATGTGGATTTCTCTC, Tyrp1 rev- AGGGAGAAAGAAGGCTCCTG, 18s fwd- AGGTTCTGGCCAACGGTCTAG, 18s rev- CCCTCTATGGGC AATTTT.

Cyclopurine quantification

Extraction of nuclear DNA from mouse skin tissues—Nuclear DNA was isolated from mouse skin using a high-salt method. Tissues were ground under liquid nitrogen into fine powder using a mortar and pestle. A nuclei lysis buffer containing 20 mM Tris (pH 8.3), 20 mM EDTA, 400 mM NaCl, 1% SDS (w/v) and 0.05% proteinase K (w/v) was added to the tissue and incubated in a water bath at 55°C overnight. Half volume of saturated NaCl solution was added to the digestion mixture, incubated at 55°C for 15 min then centrifuged at ~10,000 rpm for 30 min. The supernatant was collected and centrifuged again. The nucleic acids in the supernatant were precipitated with cold ethanol, dissolved in water and incubated in the presence of 0.03% RNase A (w/v) and 0.25 U/μL of RNase T1 at 37°C overnight, and subsequently extracted with an equal volume of chloroform/isoamyl alcohol (24:1, v/v) twice. The DNA was then precipitated from the aqueous layer by cold ethanol, centrifuged at 8,000 rpm at 4°C for 15 min, washed twice with 70% cold ethanol and dried under vacuum. The DNA pellet was dissolved in deionized water and quantified by using ultraviolet absorption spectrophotometry.

Enzymatic digestion of nuclear DNA—Nuclease P1 (16 U), phosphodiesterase 2 (0.025 U), 20 nmol of EHNA and a 30-μL solution containing 300 mM sodium acetate (pH 5.6) and 10 mM zinc chloride were added to 200 μg of DNA. In this context, EHNA served as an inhibitor for deamination of 2′-deoxyadenosine to 2′-deoxyinosine (dI) induced by adenine deaminase. The above digestion was continued at 37°C for 48 h. To the digestion mixture were then added alkaline phosphatase (10 U), phosphodiesterase 1 (0.0125 U) and 60 μL of 0.5 M Tris-HCl buffer (pH 8.9). The digestion was continued at 37°C for 2 h and subsequently neutralized by addition of formic acid. To the mixture were then added uniformly ^{15}N-labeled standard lesions, which included 400 fmol of *R*-cdG, 150 fmol of *S*-cdG, 80 fmol of *R*-cdA and 40 fmol of *S*-cdA. The enzymes in the digestion mixture were subsequently removed by chloroform extraction twice. The resulting aqueous layer was subjected to off-line high-performance liquid chromatography (HPLC) separation for the enrichment of the lesions under study, following our previously described procedures[26].

LC-MS/MS/MS Analysis—The LC-MS/MS/MS experiments were conducted using an LTQ linear ion trap mass spectrometer using our recently described conditions[26]. Briefly, the amounts of cdA and cdG lesions in each nucleoside sample were calculated based on the ratios of peak areas found in the selected-ion chromatograms for the analyte (e.g., the 23.5 min peak in the top panel of Fig. 4d for *S*-cdA) and the corresponding stable isotope-labeled standard (e.g., the 23.4 min peak in the bottom panel of Fig. 4d for the ^{15}N-labeled *S*-cdA),

the known amount of uniformly ^{15}N-labeled standard added to the nucleoside mixture (e.g., 40 fmol for *S*-cdA), and calibration curves. The calibration curves were constructed from the same LC-MS/MS/MS analyses of a series of mixtures with known compositions of the unlabeled cdA, cdG and constant amounts of the corresponding uniformly ^{15}N-labeled standards, as described previously[26]. The lesion formation frequencies as shown in Fig. 4e were then calculated by dividing the amounts of cdA and cdG in the sample with the total amount of nucleosides present.

Skin irradiation and lipid peroxide measurement

6-week old mice were euthanized and fur was removed using animal shears with a 0.25 mm head. Twelve sections of skin, each with an area of 1 cm^2, were removed from each mouse and placed in 35mm dishes on ice after adherence to Whatman filter paper suspended in PBS. For each UV and visible light study, 6 sections of skin from each mouse were placed in the dark on ice as controls. For UV studies, 6 sections of skin from each mouse were irradiated on ice with 10 J/cm^2 UVA and 0.65J/cm^2 UVB at an irradiance of 6.67 mW/cm^2 using a Sylvania 350 Blacklight (Osram Sylvania). This UV distribution is comparable to natural sunlight (96.65% UVA & 3.35% UVB). Two mice of each pigmentation type were used for a total of *n=12* skin samples for each condition. For visible light studies, 6 sections of skin from each mouse were irradiated on ice with 180 J/cm^2 visible light from a Dolan-Jenner A3200 Fiber-Lite Illuminator at an irradiance of 200 mW/cm^2. The illuminator bulb was fit with a Thorlabs FEL0400 Edgepass UV filter with a transmission of <0.001% for wavelengths <400 nm, such that no irradiation output was detectable in the UV range below 400 nm. One mouse of each pigmentation type was used for a total of 6 skin samples for each condition. Following treatment, skin sections were flash frozen and homogenized in PBS containing the antioxidant butylated hydroxytoluene (BHT) to prevent further lipid peroxidation, using a Qiagen TissueLyser II. Homogenized samples were centrifuged and supernatants were collected. Protein content of each sample was determined by Coomassie Plus Protein Assay, and samples were diluted with PBS+BHT for normalization of sample concentration (Thermo Scientific). Lipid peroxidation of each irradiated set of sample was determined using an OxiSelect TBARS Assay Kit and normalized to its unirradiated control (Cell Biolabs).

Supplementary Material

Refer to Web version on PubMed Central for supplementary material.

Acknowledgments

We thank T. Kunisada for generously sharing K14-SCF mice and C.L. Evans for help with mouse skin irradiation. We also thank A.P. Codgill for help with primary tumor cell culture and A. Piris for pathology consultation as well as M. Haigis and Z. Abdel-Malik for useful discussions. This work was supported by the following grants from the National Institutes of Health 5R01 AR043369-16 (DEF), R01-CA101864 (YW), and F30 ES020663-01 (DM), as well as support from the Dr. Miriam and Sheldon Adelson Medical Research Foundation, the US-Israel Binational Science Foundation, and the Melanoma Research Alliance (DEF).

References

1. Rhodes AR, Weinstock MA, Fitzpatrick TB, Mihm MCJ, Sober AJ. Risk factors for cutaneous melanoma. A practical method of recognizing predisposed individuals. JAMA. 1987; 258:3146–3154. [PubMed: 3312689]
2. Valverde P, Healy E, Jackson I, Rees JL, Thody AJ. Variants of the melanocyte-stimulating hormone receptor gene are associated with red hair and fair skin in humans. Nat Genet. 1995; 11:328–330. [PubMed: 7581459]
3. Rouzaud F, Kadekaro AL, Abdel-Malek ZA, Hearing VJ. MC1R and the response of melanocytes to ultraviolet radiation. Mutation research. 2005; 571:133–152. [PubMed: 15748644]
4. Wenczl E, et al. (Pheo)melanin photosensitizes UVA-induced DNA damage in cultured human melanocytes. J Invest Dermatol. 1998; 111:678–682. [PubMed: 9764853]
5. Hill HZ, Hill GJ. UVA, pheomelanin and the carcinogenesis of melanoma. Pigment Cell Res. 2000; 13 (Suppl 8):140–144. [PubMed: 11041372]
6. Curtin JA, et al. Distinct sets of genetic alterations in melanoma. N Engl J Med. 2005; 353:2135–2147. [PubMed: 16291983]
7. Elwood JM, Jopson J. Melanoma and sun exposure: an overview of published studies. International Journal of Cancer. 1997; 73:198–203.
8. Robbins LS, et al. Pigmentation phenotypes of variant extension locus alleles result from point mutations that alter MSH receptor function. Cell. 1993; 72:827–834. [PubMed: 8458079]
9. Halaban R, et al. Tyrosinases of murine melanocytes with mutations at the albino locus. Proc Natl Acad Sci U S A. 1988; 85:7241–7245. [PubMed: 3140237]
10. Vanover JC, et al. Stem cell factor rescues tyrosinase expression and pigmentation in discreet anatomic locations in albino mice. Pigment cell & melanoma research. 2009; 22:827–838. [PubMed: 19682281]
11. Kunisada T, et al. Murine cutaneous mastocytosis and epidermal melanocytosis induced by keratinocyte expression of transgenic stem cell factor. J Exp Med. 1998; 187:1565–1573. [PubMed: 9584135]
12. Dankort D, et al. Braf(V600E) cooperates with Pten loss to induce metastatic melanoma. Nat Genet. 2009; 41:544–552. [PubMed: 19282848]
13. Patton EE, et al. BRAF mutations are sufficient to promote nevi formation and cooperate with p53 in the genesis of melanoma. Curr Biol. 2005; 15:249–254. [PubMed: 15694309]
14. Goel VK, et al. Melanocytic nevus-like hyperplasia and melanoma in transgenic BRAFV600E mice. Oncogene. 2009; 28:2289–2298. [PubMed: 19398955]
15. Michaloglou C, et al. BRAFE600-associated senescence-like cell cycle arrest of human naevi. Nature. 2005; 436:720–724. [PubMed: 16079850]
16. Dhomen N, et al. Oncogenic Braf induces melanocyte senescence and melanoma in mice. Cancer Cell. 2009; 15:294–303. [PubMed: 19345328]
17. Rae J, et al. (V600E)Braf::Tyr-CreERT2::K14-Kitl Mice Do Not Develop Superficial Spreading-Like Melanoma: Keratinocyte Kit Ligand Is Insufficient to “Translocate” (V600E)Braf-Driven Melanoma to the Epidermis. Journal of Investigative Dermatology. 132:488–491. [PubMed: 22113477]
18. D’Orazio JA, et al. Topical drug rescue strategy and skin protection based on the role of Mc1r in UV-induced tanning. Nature. 2006; 443:340–344. [PubMed: 16988713]
19. Boni A, et al. Selective BRAFV600E inhibition enhances T-cell recognition of melanoma without affecting lymphocyte function. Cancer Research. 70:5213–5219. [PubMed: 20551059]
20. Kadekaro AL, et al. Melanocortin 1 receptor genotype: an important determinant of the damage response of melanocytes to ultraviolet radiation. FASEB J. 2010; 24:3850–3860. [PubMed: 20519635]
21. Noonan FP, et al. Melanoma induction by ultraviolet A but not ultraviolet B radiation requires melanin pigment. Nat Commun. 2012; 3:884. [PubMed: 22673911]
22. Nofsinger JB, Liu Y, Simon JD. Aggregation of eumelanin mitigates photogeneration of reactive oxygen species. Free Radical Biology and Medicine. 2002; 32:720–730. [PubMed: 11937298]

23. Kovacs D, et al. The Eumelanin Intermediate 5,6-Dihydroxyindole-2-Carboxylic Acid Is a Messenger in the Cross-Talk among Epidermal Cells. Journal of Investigative Dermatology. 10.1038/jid.2011.457

24. Wang J, et al. Quantification of Oxidative DNA Lesions in Tissues of Long-Evans Cinnamon Rats by Capillary High-Performance Liquid Chromatography Tandem Mass Spectrometry Coupled with Stable Isotope-Dilution Method. Analytical Chemistry. 2011; 83:2201–2209. [PubMed: 21323344]

25. Wang Y. Bulky DNA lesions induced by reactive oxygen species. Chemical research in toxicology. 2008; 21:276–281. [PubMed: 18189366]

26. Jaruga P, Dizdaroglu M. 8,5′-Cyclopurine-2′-deoxynucleosides in DNA: Mechanisms of formation, measurement, repair and biological effects. DNA Repair. 2008; 7:1413–1425. [PubMed: 18603018]

27. Yuan B, Wang J, Cao H, Sun R, Wang Y. High-throughput analysis of the mutagenic and cytotoxic properties of DNA lesions by next-generation sequencing. Nucleic Acids Research. 2011; 39:5945–5954. [PubMed: 21470959]

28. Neugut AI, Kizelnik-Freilich S, Ackerman C. Black-white differences in risk for cutaneous, ocular, and visceral melanomas. Am J Public Health. 1994; 84:1828–1829. [PubMed: 7977927]

29. Green AC, Williams GM, Logan V, Strutton GM. Reduced melanoma after regular sunscreen use: randomized trial follow-up. Journal of Clinical Oncology. 29:257–263. [PubMed: 21135266]

30. Huncharek M, Kupelnick B. Use of topical sunscreens and the risk of malignant melanoma: a meta-analysis of 9067 patients from 11 case-control studies. Am J Public Health. 2002; 92:1173–1177. [PubMed: 12084704]

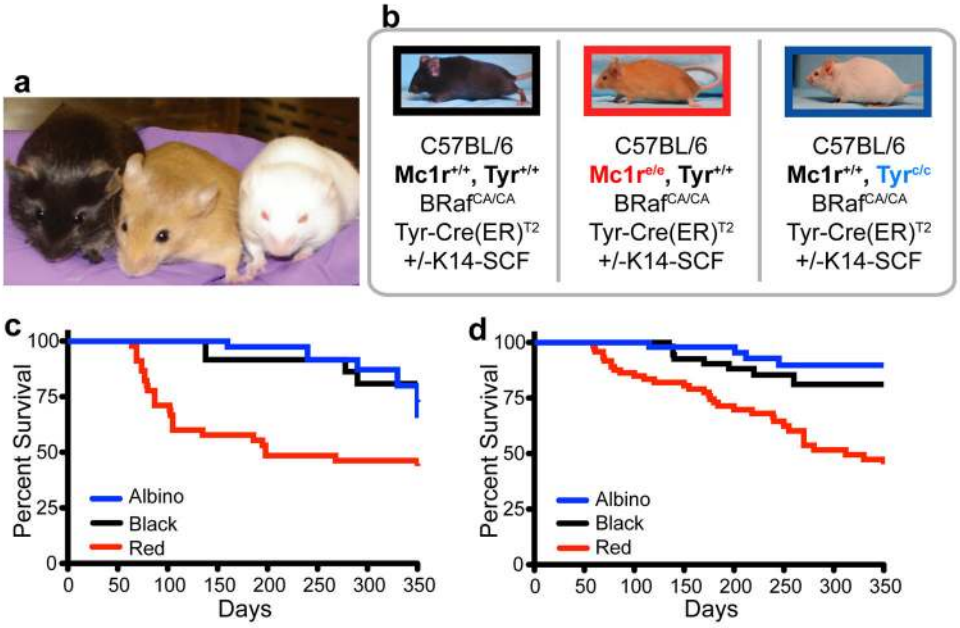

Figure 1. Without UV radiation, BRaf^{CA} red mice have an increased rate of melanoma development relative to black and albino BRaf^{CA} animals

(a) C57BL/6 pigmentation variants with epidermal melanocytes (*K14-SCF*). From left to right: black (wild-type), red (*Mc1r$^{e/e}$*), and albino (*Tyr$^{c/c}$*). (**b)** Genotype of animals used for experimental studies. (**c)** Percent survival of pigmentation variants not carrying the *K14-SCF* transgene, *i.e.* no epidermal melanocytes. (n_{black}=28, n_{red}=40, n_{albino}=48) $p_{black\text{-}albino}$=0.250, $p_{black\text{-}red}$=0.003, $p_{albino\text{-}red}$=0.003. **(d)** Percent survival of pigmentation variants carrying the *K14-SCF* transgene, *i.e.* epidermal melanocytes (n_{black}=49, n_{red}=77, n_{albino}=41) $p_{black\text{-}albino}$=0.103, $p_{black\text{-}red}$=0.009, $p_{albino\text{-}red}$<0.0001.

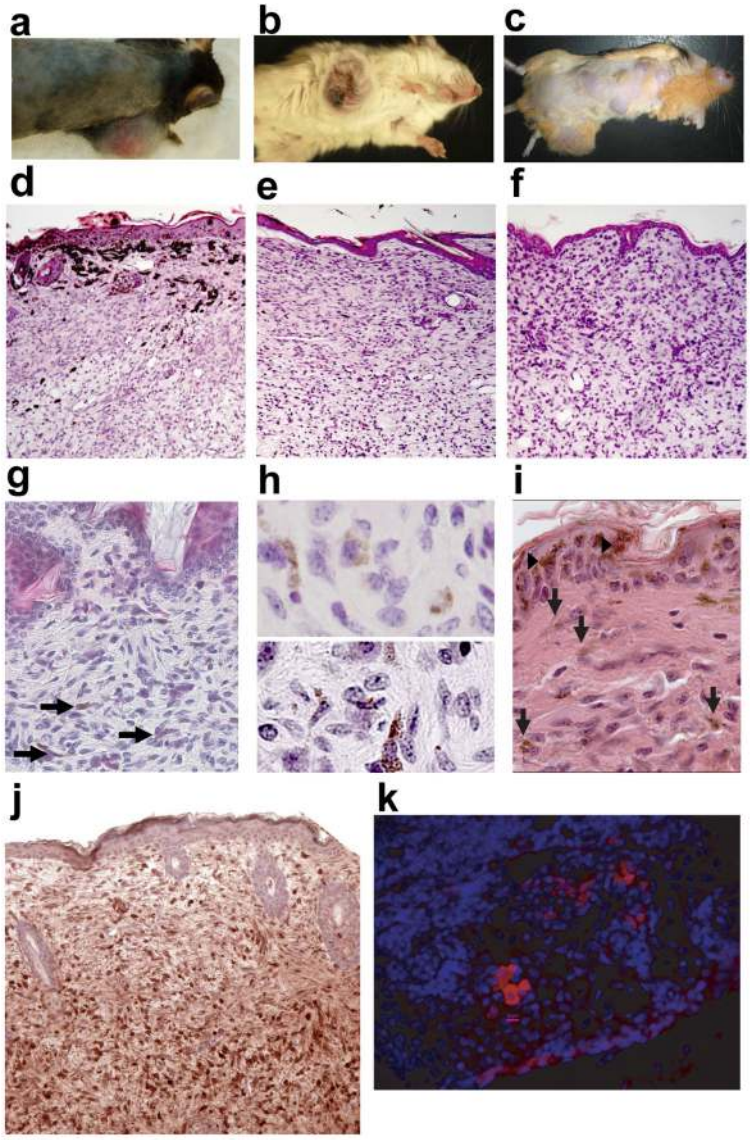

Figure 2. Melanomas on all three pigmentation variants are morphologically similar and exhibit common histologic features

Melanomas on **(a)** black, **(b)** albino, and **(c)** red mice are grossly amelanotic. Histologically, **(d)** black, **(e)** albino, and **(f)** red melanomas are also mostly amelanotic though superficial tumor cells in black-BRaf^{V600E} tumors carry melanin. **(g)** Red-BRaf^{V600E} melanomas also can carry pigment (arrows). **(h)** Further magnification of two red melanomas also illustrates pigmented tumor cells. **(i)** Forskolin induces epidermal pigmentation (arrowheads) and mild tumor cell pigmentation (arrows). **(j)** Tumor cells stain positive for S100. **(k)** Skin-draining lymph nodes carry gp100+ cells (red).

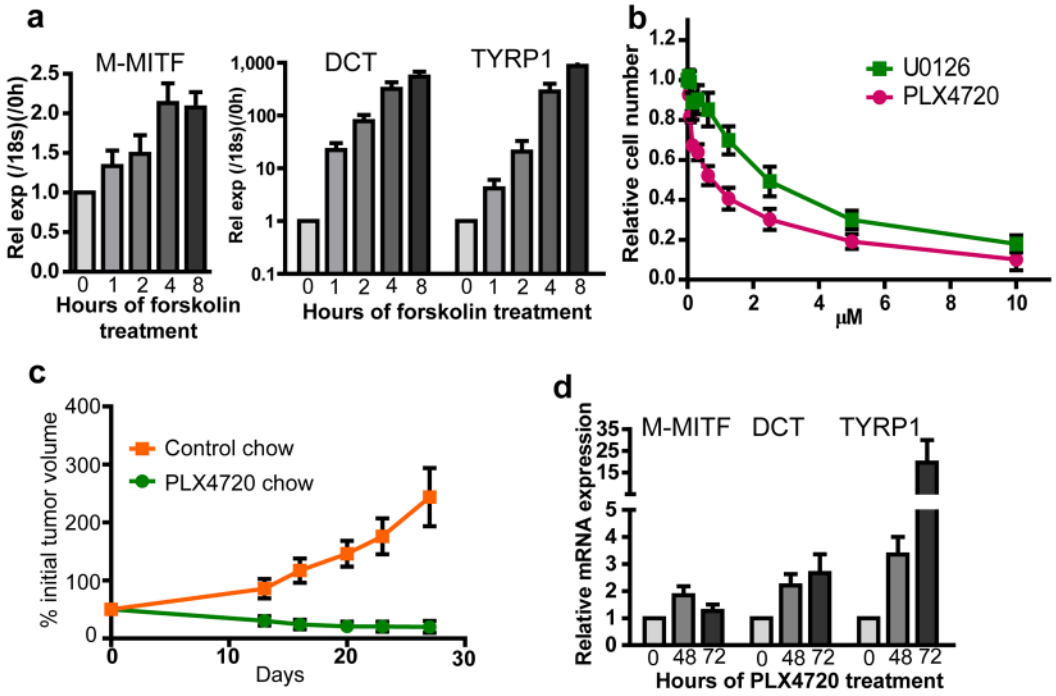

Figure 3. Tumor cells from a red-BRaf^{CA} animal behave like classic BRAF^{V600E} melanomas after cAMP upregulation or BRAF inhibition

(a) 20 μM forskolin upregulates expression of melanocytic markers (*n*=4). **(b)** MAPK inhibition by PLX4720 or U0126 decreases melanoma cell proliferation (GI^{50}_{PLX}=0.5 μM, GI^{50}_{U0126}=2 μM) (*n*=3). **(c)** PLX4720 blocks melanoma growth *in vivo* (*n*=3). **(d)** 2 μM PLX4720 upregulates expression of melanocytic markers. mRNA expression normalized to 18s rRNA and 0 h time-point. Error bars denote s.e.m.

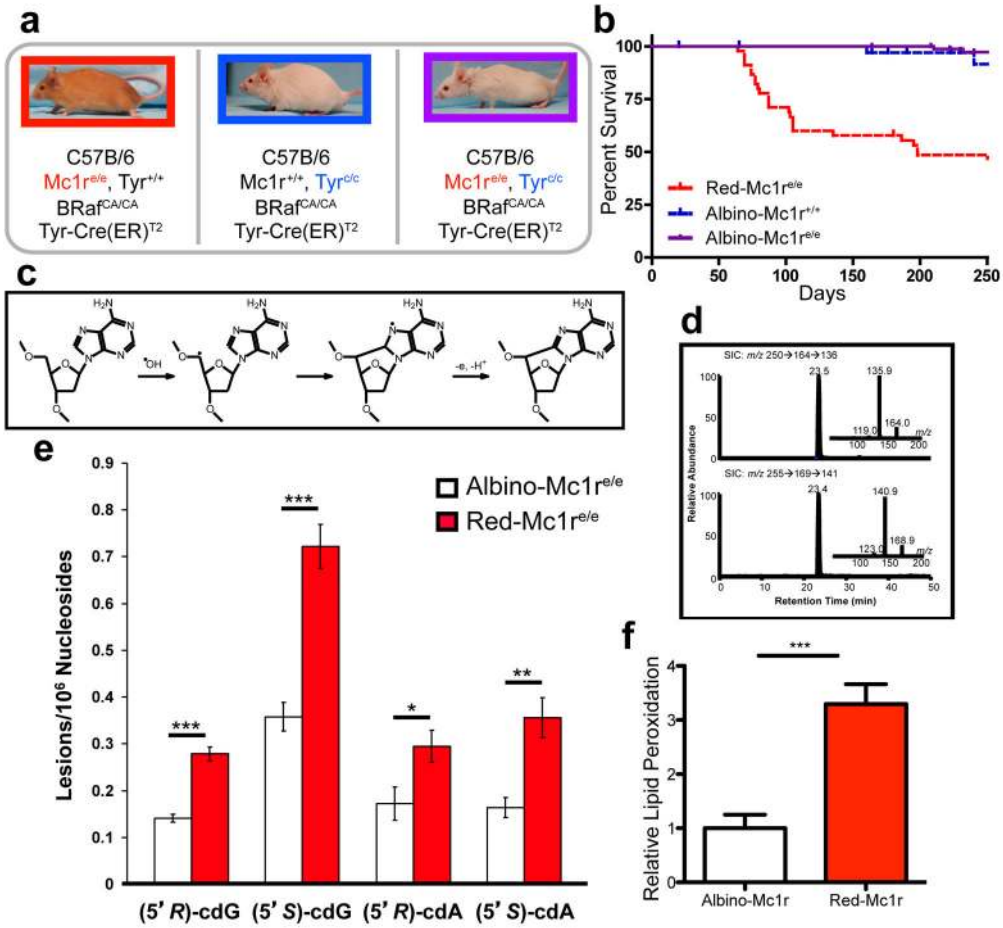

Figure 4. The UV-independent propensity of red BRaf^{CA} mice to develop melanoma is dependent on pigment production

(a) Genotypes of mice studied. **(b)** The albino allele protects *Mc1r$^{e/e}$* mice from melanoma development (n_{red}=40, n_{albino}=48, $n_{albino\text{-}red}$=90) $p_{albino/albino\text{-}red}$=0.308, $p_{albino/red}$<0.0001, $p_{red/albino\text{-}red}$<0.0001. **(c)** ROS reacts with purine nucleosides to produce 8,5′-cyclopurine lesions (cdA shown). **(d)** Selected-ion chromatograms for DNA from albino-Mc1r$^{e/e}$ mouse skin. The insets show the positive-ion MS^3 spectra for unlabeled and labeled *S*-cdA. **(e)** Both diastereomers of cdA and cdG are significantly higher in red-*Mc1r$^{e/e}$* skin. (n=3) *=p<0.05; **=p<0.01; ***=p<0.001. **(f)** Lipid peroxide levels are significantly higher in red-*Mc1r$^{e/e}$* skin (n=3). p<0.0001.